*Fibers and Polymers* 2015, Vol.16, No.8, 1781-1787
DOI 10.1007/s12221-015-5185-1

ISSN 1229-9197 (print version)
ISSN 1875-0052 (electronic version)

# Mechanical and Biological Properties of Silk Fibroin/Carbon Nanotube Nanocomposite Films

**Caixia Pan, Qifan Xie, Zeyun Hu, Mingying Yang, and Liangjun Zhu***

*Institute of Applied Bioresource Research, College of Animal Science, Zhejiang University, Hangzhou 310058, China*
(Received March 11, 2015; Revised May 31, 2015; Accepted June 5, 2015)

**Abstract:** Multi-walled carbon nanotubes (MWCNTs) were homogeneously dispersed in silk fibroin (SF) solutions at different compositions, and a simple solvent-casting method was used to fabricate SF/MWCNT films. Structure, viscosity, and mechanical properties of the SF/MWCNT nanocomposites were characterized by FTIR (Fourier Transform Infrared Spectroscopy), viscometry, and tensile testing. Fibroblast cells were used to examine cell viability and attachment to nanocomposite films. Compared to a pure SF film, adding just 0.5 % (w/w) of MWCNT to the SF matrix could enhance the Young's modulus and ultimate tensile strength by approximately 24 % and 39 %, respectively. In addition, with increasing MWCNTs content, the percentage of $\beta$-sheet structure increased significantly. When the content of MWCNTs increased from 0 to 1 % (w/w), the $\beta$-sheet content improved from 17.8 % to 53.6 %. Furthermore, adding up to 1 % (w/w) MWCNT increased the viscosity of the SF solution ten fold. From a biological point of view, no toxic effect was observed on fibroblast cells in the presence of MWCNTs after 3 and 7 days. This investigation suggests that SF/MWCNT nanocomposite films with improved mechanical properties and biocompatibility are well-suited as novel biomaterials.

**Keywords:** Silk fibroin, Multi-walled carbon nanotubes, Nanocomposites, Mechanical properties, Biocompatibility

## Introduction

The necessity to optimize the design of tissue engineering scaffolds has led to the progress of biomaterial composites with unexceptional properties [1,2]. Following the discovery of the carbon nanotube (CNT) in 1991 [3], these nanosized materials have quickly become a technological platform for diverse fields of research, including materials and biomedical engineering. CNTs are one of the most useful nanoscale agents for material property reinforcement because of their extraordinary mechanical, electrical, and thermal properties [4-6]. CNTs have shown controversial and complex properties. Pristine CNTs have displayed cytotoxicity on certain cell lines, which can be attributed to the use of metal catalysts, such as nickel, during CNT fabrication [7]. Conversely, CNTs incorporated with biopolymers have shown great biocompatibility [8-10]. Despite the growing debate over the cytotoxicity of CNTs, these previous publications demonstrate why interest in this field has doubled in recent years [11].

Silk is a natural protein that has been widely used as a biomaterial for many years. Due to its flexible nature, biocompatibility, and *in vivo* reabsorbing and water-dissolvable properties, the silk fibroin (SF) protein has been used as a scaffold material in various tissue engineering applications [12-14]. In addition, diverse forms of SF, such as microparticles [15], films [16], and gels [17], have been developed. SF/CNT composites were previously used for biosensor applications [18], and recently have been proposed as materials for effective neuronal cell transplantation in CNT-based scaffold fabrication [19,20]. Despite the advantageous properties of SF mentioned above, SF demonstrates poor mechanical properties when it is not cross-linked. Therefore, CNTs have also been used for improving mechanical properties in recent studies [21,22].

To date, many relevant literatures investigates either cell compatibility [19,20] or the material properties [21,22] of SF/CNT composites. Considering the capabilities of CNTs as additives, the aim of this study is to present a comprehensive investigation of SF/CNT nanocomposite films fabricated by a simple procedure. Second structures, mechanical properties, and cell cytotoxicities of films were characterized to better understand the interactions between silk fibroin and CNTs. Multi-walled carbon nanotubes (MWCNTs) were selected to reinforce the SF matrix because MWCNTs have been proven to be more beneficial in biomedical engineering applications than single-walled carbon nanotubes (SWCNTs) [23,24].

## Experimental

### Materials

Bombyx mori cocoons were purchased from Shandong Academy of Sericulture, China. Muti Wall Carbon nanotubes (MWCNTs, Main Range of Diameter: 10-20 nm; Length: <2 um; Special Surface Area: 100-160 $m^2$/g.) were purchased from Shenzhen Nanotech Port Co. Ltd., China. $Na_2CO_3$, PBS, LiBr, and other reagents of analytical grade were purchased from Sinopharm Chemical Reagents Co. Ltd., China. Deionized (DI) water was used throughout all experiments. Fetal bovine serum (FBS) and 0.25 % trypsin were purchased from Invitrogen. Dulbecco's modified Eagle's medium (DMEM) and 1 % penicillin-streptomycin were purchased from Gibco.

*Corresponding author: ljzhu@zju.edu.cn

**Silk Fibroin Purification**

Aqueous silk fibroin stock solutions were prepared as described previously [25]. In brief, cocoons of Bombyx mori were boiled for 1 h in an aqueous solution of 0.02 M sodium carbonate and then rinsed thoroughly with DI water. After drying, the extracted silk fibroin was dissolved in 9.3 M LiBr solution at 60 °C for 4 h, yielding a 20 % (w/v) solution. The solution was dialyzed against DI water in a Slide-a-Lyzer dialysis cassette (MWCO, 8000, Pierce) for 3 days to remove salt impurities. The solution was optically clear after dialysis and was centrifuged to remove small amounts of silk aggregate formed during the process. The final concentration of the aqueous SF solution was ~8 % (w/v). This concentration was determined by weighing the residual solid of a known volume of solution after drying.

**SF/MWCNT Nanocomposite Film Fabrication**

MWCNTs were added into purified SF solution at weight ratio of 0, 0.1, 0.5, and 1 %(w/w). After blending, each sample was sonicated with a high power sonic tip (180 W) for 20 min, followed by 2 h in a mild sonication bath. The viscosity and dispersion quality of each solution were analyzed. A portion of each prepared solution was added to a glass vial to examine the homogeneity and stability after keeping at a stationary position for 3 days. To fabricate SF/MWCNT films, the solutions of different MWCNTs compositions were poured into Petri dishes and dried at room temperature in a laminar-flow hood overnight. Dried, uniform, thin films with an average thickness of 0.10 mm (measured by calipers) were easily removed from the petri dishes.

**Viscosity and Dispersion Quality**

To determine the effect of MWCNTs on the viscosity of SF, SF/MWCNT solutions were poured into the measuring cylinders of a viscometer (SNB, Ni Run, China).Viscosity tests were performed at room temperature at a rotor speed of 60 RPM. The dispersion quality of each SF/MWCNT solutions was detected by a spectrophotometer (UV-2450, Shimadzu, Japan), demonstrating the homogeneity and stability of the mixed solutions.

**Fourier Transform Infrared (FT-IR) Spectroscopy**

Secondary protein structures, including random coils, $\alpha$-helices, $\beta$-sheets, and turns, were evaluated using their infrared absorbance spectra. Analysis of the infrared spectrum covering the amide I region (1595-1705 $cm^{-1}$) was performed by Origin 8.5 software. Absorption bands in the wavenumber ranging from 1616 to 1637 $cm^{-1}$ and 1695 to 1705 $cm^{-1}$ represent enriched $\beta$-sheet structures. Bands in the range of 1638-1655 $cm^{-1}$ were ascribed to random coil structures. Bands in the range of 1656-1663 $cm^{-1}$ were ascribed to $\alpha$-helices, and bands in the range of 1663-1695 $cm^{-1}$ were ascribed to turns [26]. FT-IR spectra of the films were obtained at room temperature with an FTIR spectrometer (FT-IR-8400S, Shimadzu, Japan). Background measurements were collected with an empty cell and subtracted from each sample spectrum. For each measurement, 40 scans were recorded with a resolution of 4 $cm^{-1}$, and the wave number ranged from 400 to 4000 $cm^{-1}$.

**Mechanical Properties**

The tensile properties of pure and MWCNT-filled silk fibroin films were determined using a universal testing machine (AGS-J, Shimadzu, Japan), fit with a 50 N load cell. The films were peeled from the petri dish and cut into strips measuring 30 mm×8 mm. The thickness of each strip was measured with a low torque digital micrometer. Strips were held by two grips in the instrument. The test speed was set to 2 mm/min. For each composition, stress-strain measurements were conducted on five strips. From each set of five measurements, the mean and standard error were calculated for the Young's modulus, ultimate tensile strength, strain to failure, and yield strength.

**Biocompatibility Evaluation**

Fibroblast cells were expanded in a growth medium containing 90 % DMEM, 10 % FBS, 100 U/m*l* penicillin, and 1000 U/m*l* streptomycin. Cell cultures were maintained at 37 °C in an incubator with 95 % air and 5 % $CO_2$. The cultures were replenished with fresh medium at 37 °C every 2 days. For adhesion experiments, cells were seeded on silk films that were precast in 96-well plates with 500 cells per well in 100 $\mu l$ of serum-containing medium. To evaluate cell attachment, 10 $\mu l$ of alamar blue (Alamar Blue Kit, Fanbo biochemicals Co. Ltd., China) was added to the culture medium after 3 h of cell seeding, and the medium fluorescence (Ex=560 nm, Em=590 nm) was determined after 6 h of culture in a 5 % $CO_2$ incubator at 37 °C. After 3 and 7 days of culture, cell proliferation was also determined by alamar blue, as mentioned above. Cell numbers were correlated to the fluorescence values. In addition, after cultures of 3 and 7 days, cell morphologies were observed by adding specimens to a 4 % formalin solution for 15 min and a 1 % Triton X-100 in PBS for 10 min. The cytoskeletons were visualized by actin (F-actin was detected using TRITC-conjugated Phalloidin; Millipore) under a confocal microscope (FV1000, Olympus, Japan).

## Results and Discussion

**Homogeneity and Stability**

MWCNTs have poor wetting properties in water such that they aggregate and precipitate out of suspension. Figure 1(A) demonstrates how, after only 1 h, a water/MWCNT dispersion of the same concentration as the middle sample (0.5 wt %) shows aggregation and precipitation. Generally, MWCNTs were found at the air/water interface, a behavior caused by the combination of the MWCNT's large aspect

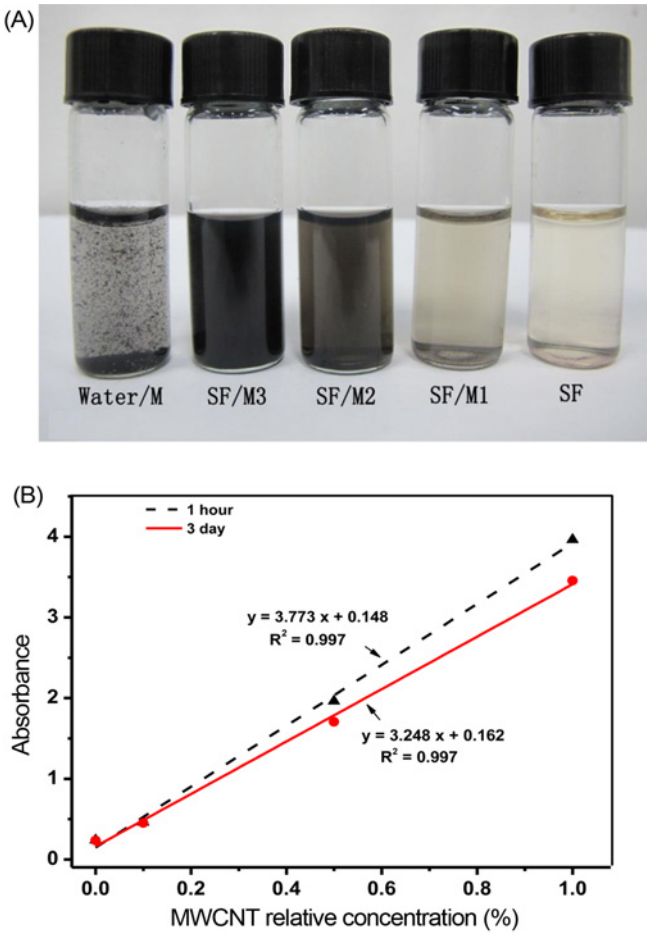


**Figure 1.** (A) SF/MWCNT nanocomposite solutions of different MWCNT compositions (M1, M2, M3 represent 0.1 % (w/w) MWCNT, 0.5 % (w/w) MWCNT, 1 % (w/w) MWCNT respectively.) after 3 days, and MWCNTs in water (Water/M) after only 1 h. (B) Absorbance of SF/MWCNT solutions as a function of relative MWCNT concentration of after 1 h and 3 days in a stationary position.

ratio and water's high surface tension. All other solutions containing any quantity of SF demonstrate improved MWCNTs dispersion after 3 days, suggesting that the SF stabilizes MWCNTs in water. At higher MWCNTs compositions, the dispersions approached an opaque, black color. These compositions were completely stable, and no degradation, separation, or flocculation was observed after 1 month of visual tracking. As show in Figure 1(B), linear relationships were observed between MWCNTs composition and UV absorbance after 1 h and 3 days of stationary solutions, which was in agreement with previous work [27,28]. Furthermore, the linear trend is typically attributed to the rich dispersion of CNTs [29]. These data also indicated that MWCNTs were stable and uniformly dispersed in silk fibroin solutions.

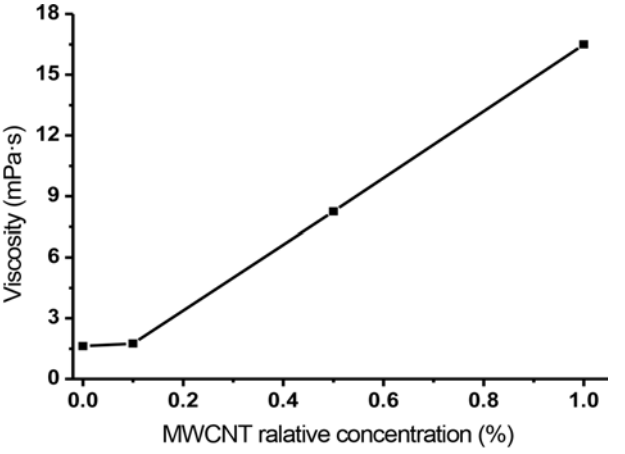


**Figure 2.** The relationship between viscosity and MWCNT concentration.

**Viscosity**

Silk fibroin and SF/MWCNT nanocomposite solutions have recently been used to electrospin SF nanofibers [30]. As an important property for electrospinning, the viscosity of each prepared solution was measured by a viscometer. Figure 2 presents the effect of MWCNTs content on the solution viscosity. The addition of up to 0.1 % MWCNTs did not have a remarkable effect on the viscosity. However, by increasing the MWCNTs content, solution viscosity could be increased. Adding 1 % MWCNTs into the SF solution increased the viscosity ten fold. This phenomenon could be explained by the interaction between the SF/MWCNT solution and the rotor wall. Nano-sized carbon particles and cylinders are prone to attach to the rotor wall due to Van der Waals forces.

**Secondary Structure of SF/MWCNT Films**

In order to know how MWCNTs effect on silk fibroin structure, the secondary structures of the films were investigated by FT-IR spectroscopy. According to the analysis by origin 8.5 software, the infrared spectrums of different MWCNTs contents blended silk films covering the amide I region (1595-1705 $cm^{-1}$) were performed (Figure 3(A)-(D)). Silk fibroin contains four types of secondary structure: random coils, $\alpha$-helices, $\beta$-sheets, and $\beta$-turns. The quantities of these structures in fibers play an important role in the mechanical properties. As shown in Figure 3(E,F,G,H), when the concent of MWCNTs increased from 0 to 0.1 % (w/w), the percentage of $\beta$-sheets increased while $\beta$-turn structures decreased significantly ($p$<0.01). With the increase of MWCNTs concent to 0.5 % (w/w), the percentage of $\beta$-sheets and $\beta$-turn continued to change, meanwhile, the percentage of $\alpha$-helices and random coils decreased significantly (P<0.01). When the MWCNTs concent reached 0.5 % (w/w), the $\beta$-sheet structure increased from 32.77 %

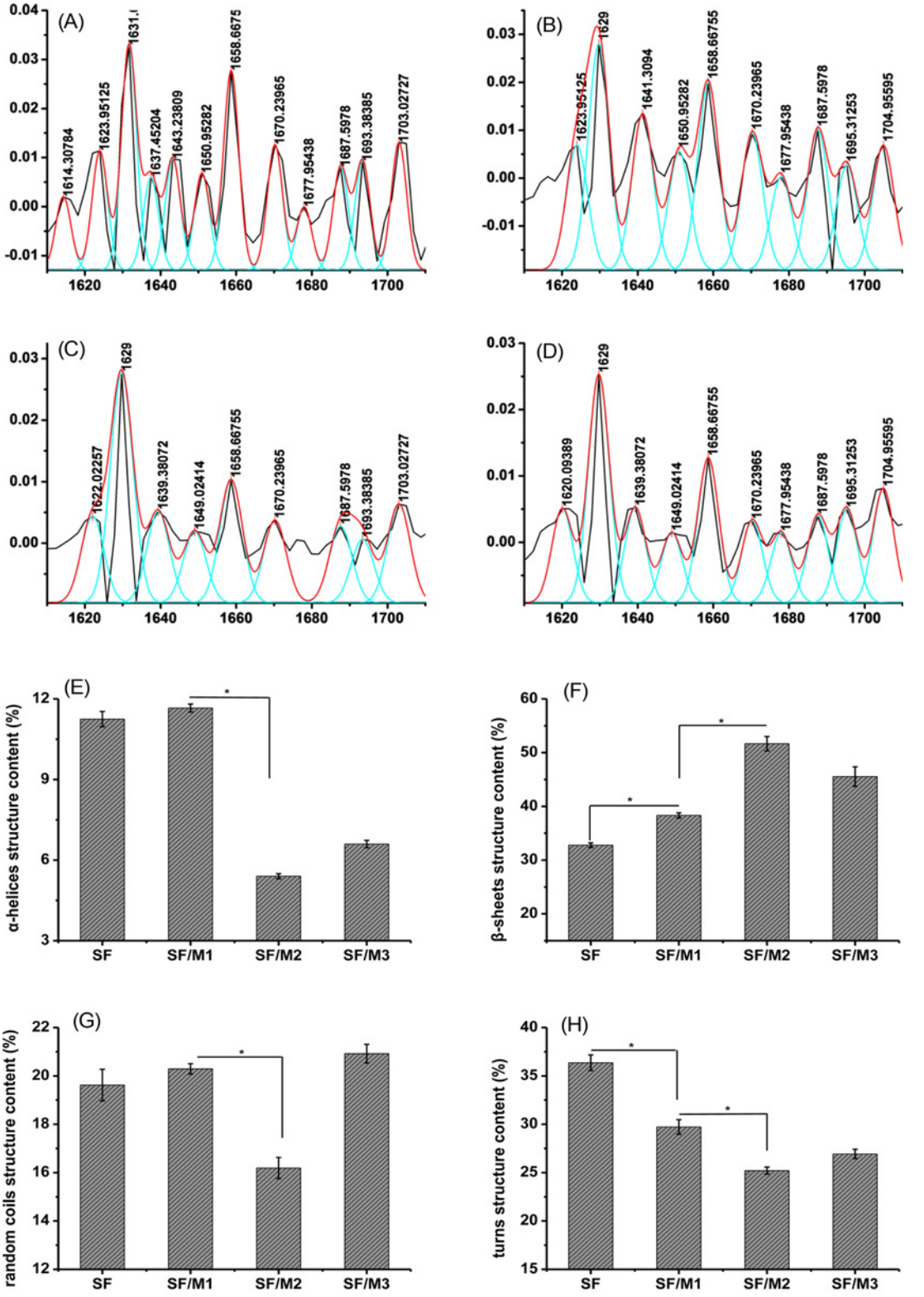


**Figure 3.** FT-IR spectra and secondary structure contents of silk films fabricated at various MWCNT concentration; (A) FT-IR spectra of SF (pure silk film), (B) FT-IR spectra of SF/M1 (SF/0.1 % (w/w) MWCNT film), (C) FT-IR spectra of SF/M2 (SF/0.5 % (w/w) MWCNT film), (D) FT-IR spectra of SF/M3 (SF/1 % (w/w) MWCNT film), (E) $\alpha$-helices structure content, (F) $\beta$-sheets structure content, (G) random coils structure content, and (H) turns structure content. *Significant difference between groups (*$p$<0.01). The data represent mean±SD ($n$=4).

to 51.67 %, and $\beta$-turn decreased from 36.36 % to 25.21 %. This indicated that even a small addition of MWCNTs to the aqueous SF solution resulted in a significant conformation transition of silk fibroin, from an intermediate conformation to $\beta$-sheets. However, it was noticed that, when the content of MWCNTs reached to 1 % (w/w), the percentage of $\beta$-sheet decreased, but $\alpha$-helices, random coils and $\beta$-turns increased. The discontinuousness may be attributed to the MWCNTs aggregation.

**Mechanical Properties of SF/MWCNT Films**

To investigate the effects of MWCNTs concentration on the mechanical properties of SF films, tensile testing was performed at room temperature. The Young's moduli (Y), strains at break ($\varepsilon$), ultimate strengths (US), and yield strengths (YS) of pure and nanocomposite SF films are shown in Figure 4. Small additions of MWCNTs to SF led to effictive improvements for mechanical properties. Furthermore, compared to pure SF films, nanocomposite films with 0.5 % (w/w) MWCNTs exhibited a 24 % increase in the Young's modulus, a 34 % increase in the strain at break, a 39 % increase in the ultimate tensile strength, and a 30 % increase in the yield strength. The mechanical improvements of these SF films by MWCNT inclusion could be attributed to the interaction between reinforcing MWCNT particles dispersed in an SF matrix. Because of the strong interactions between SF and MWCNTs, more energy was needed to overcome the molecular bonding energy, leading to an increase in Young's modulus and tensile strength. Meanwhile, well-dispersed MWCNTs in silk films induced an increase in $\beta$-sheet content, which might also contribute to the mechanical improvement of the films. However, it was worth noting that upon increasing the MWCNTs concentration further, Young's modulus only increased modestly while tensile strength, yield strength and elongation tended to decrease slightly. The reduction of mechanical improvement could be caused by MWCNTs aggregation at high concentrations. This result was consistent with the secondary structure changes of composite films mentioned above. Moreover, after reaching an energy threshold, nanocracks began to emerge at the MWCNT-SF interfaces, finally resulting in the tensile failure at lower elongations and tensile strengths with no significant improvement in Young's modulus of 1 % (w/w) SF/MWCNT films.

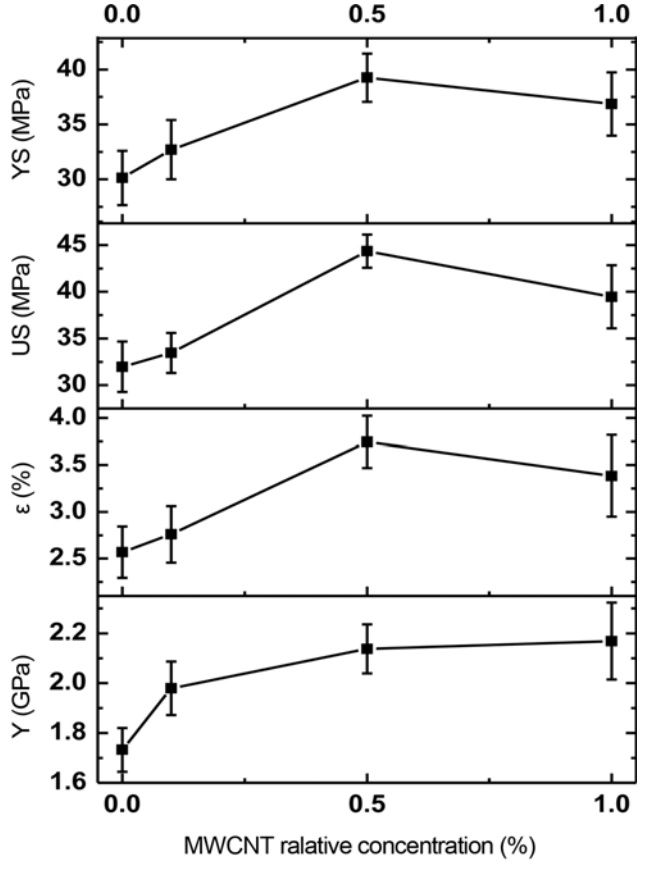


**Figure 4.** Yield strengths (YS), ultimate tensile strengths (US), strains to failure ($\varepsilon$), and Young's moduli (Y) of SF/MWCNT films of various MWCNT concentrations. The data represent mean±SD ($n$=5).

**Biocompatibility of SF/MWCNT Films**

As observed from Figure 5(A), after 3 days of cell culture, the cells could proliferate and attach to all kinds of film surfaces, showing a good cytocompatibility of the films. At this time point, the majority of the cells were not completely elongated and did not well distributed. Moreover, after 7 days the cells altered to elongated morphology, and the number of the cells significantly increased.

Certain parts of the images in Figure 5(A) are not very clear due to surface roughness on the micrometer scale. Figure 5(B) shows that initial cell attachment after 3 h was similar on all four surfaces, as quantified by alamar blue. After 3 and 7 days of culturing, the fluorescence values of SF, SF/M1 and SF/M2 were at a similar level with no significant difference between them. While the value of SF/M3 was small obviously. expecially after 7 days of culturing, there was significant difference ($p$<0.05, Figure 5(C)) compared with SF/M2. This result indicated that high MWCNTs concentrations were less favorable for the growth of fibroblast cells. It was also possibly result in MWCNTs aggregated on SF/M3 (last row in Figure 5(A)), which was not conducive to the growth of cells. Overall, fibroblast cells adhered strongly and proliferated over 3 and 7 days on all nanocomposite surfaces indicating the nontoxic effects of MWCNTs. Further studies are still necessary to verify the biocompatibility for specific applications.

## Conclusion

This study investigated the structures, mechanical properties,

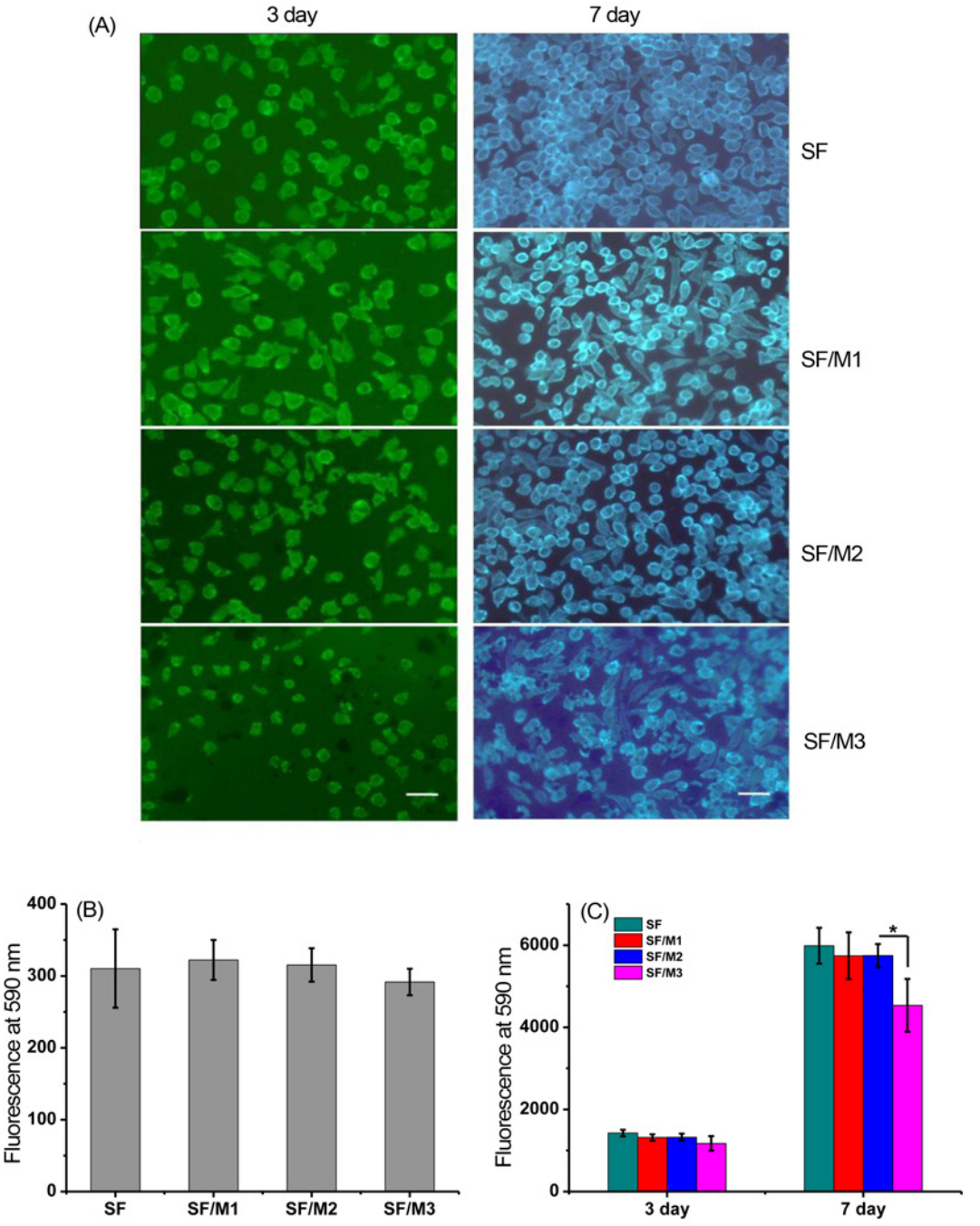


**Figure 5.** Attachment and proliferation of fibroblast cells on nanocomposite surfaces; (A) microscopic images of cultured fibroblast cells on SF (pure silk film), SF/M1 (SF/0.1 % (w/w) MWCNT film), SF/M2 (SF/0.5 % (w/w) MWCNT film) and SF/M3 (SF/1 % (w/w) MWCNT film) after 3 days and 7 days, (B) 3 h attachment of fibroblast cells on nanocomposite films, and (C) 3 day and 7 day proliferation of fibroblast cells on nanocomposite films. *Significant difference between groups (*$p$<0.05). The data represent mean±SD ($n$=4).

viscosities, and biological properties of SF/MWCNT nanocomposites. By using a simple fabrication method, we obtained homogeneous dispersions of MWCNTs in a SF matrix. Adding low concentrations of MWCNTs had significant effects on secondary structure, viscosity, and mechanical properties. Adding 0.5 % (w/w) MWCNTs to the SF matrix enhanced the Young's modulus and ultimate tensile strength by approximately 24 % and 39 %, respectively. With increasing MWCNTs concentration from 0 to 1 % (w/w), the percentage of $\beta$-sheet structure increased significantly from 17.8 % to

53.6 %. Fibroblast cells' attachment and proliferation on nanocomposite surfaces were also studied. No cell toxicity effect was observed after 3 and 7 days. In summary, it was shown that SF/MWCNT nanocomposite films with enhanced mechanical and biocompatibility are well-suited as novel biomaterials.

## Acknowledgements

This study is supported by the earmarked fund (CARS-22-ZJ0402) for China Agriculture Research System (CARS) and National Natural Science Foundation of China (21172194).

## References

1. A. K. Mohanty, M. Misra, and G. Hinrichsen, *Macromol. Mater. Eng.*, **276**, 1 (2000).
2. R. A. MacDonald, B. F. Laurenzi, G. Viswanathan, P. M. Ajayan, and J. P. Stegemann, *Biomed. Mater. Res. A.*, **74**, 489 (2005).
3. S. Iijima, *Nature*, **354**, 56 (1991).
4. M. Shokrieh and R. Rafiee, *Mech. Compo. Mater.*, **46**, 155 (2010).
5. A. A. Balandin, *Nat. Mater.*, **10**, 569 (2011).
6. R. A. MacDonald, C. M. Voge, M. Kariolis, and J. P. Stegemann, *Acta Biomater.*, **4**, 1583 (2008).
7. S. Agarwal, X. Zhou, F. Ye, Q. He, G. C. Chen, J. Soo, F. Boey, H. Zhang, and P. Chen, *Langmuir*, **26**, 2244 (2010).
8. S. K. Misra, F. Ohashi, S. P. Valappil, J. C. Knowles, I. Roy, S. R. P. Silva, V. Salih, and A. R. Boccaccini, *Acta Biomater.*, **6**, 735 (2010).
9. J. E. Tercero, S. Namin, D. Lahiri, K. Balani, N. Tsoukias, and A. Agarwal, *Mater. Sci. Eng. C-Mater. Biol. Appl.*, **29**, 2195 (2009).
10. A. Lobo, E. Antunes, A. Machado, C. Pacheco-Soares, V. Trava-Airoldi, and E. Corat, *Mater. Sci. Eng. C-Mater. Biol. Appl.*, **28**, 264 (2008).
11. B. S. Harrison and A. Atala, *Biomaterials,* **28**, 344 (2007).
12. G. H. Altman, F. Diaz, C. Jakuba, T. Calabro, R. L. Horan, J. Chen, H. Lu, J. Richmond, and D. L. Kaplan, *Biomaterials*, **24**, 401 (2003).
13. U. J. Kim, J. Park, H. J. Kim, M. Wada, and D. L. Kaplan, *Biomaterials,* **26**, 2775 (2005).
14. Y. Wang, H. J. Kim, G. Vunjak-Novakovic, and D. L. Kaplan, *Biomaterials,* **27**, 6064 (2006).
15. J. Qu, Y. Liu, Y. Yu, J. Li, and J. Luo, *Mater. Sci. Eng. C-Mater. Biol. Appl.*, **44**, 166 (2014).
16. J. D. White, S. Wang, A. S. Weiss, and D. L. Kaplan, *Acta Biom.*, **14**, S1742-7061-00548-0 (2014).
17. X. Wang, B. Partlow, J. Liu, Z. Zhang, and B. Su, *Acta Biom.*, **14**, S1742-7061-00469-3 (2014).
18. J. Liu, X. Zhang, H. Pang, B. Liu, and Q. Zou, *Biosens. Bioelectron.*, **15**, 31 (2012).
19. C. Chi-Shuo, S. Sushant, and L. Catherine, *Nanoscale Res. Lett.*, **7**, 126 (2012).
20. S. Y. Cho, Y. S. Yun, E. S. Kim, M. S. Kim, and H. J. Jin, *Nano. Nanotechnol.*, **5**, 801 (2011).
21. D. Blond, D. N. McCarthy, W. J. Blau, and J. N. Coleman, *Biomacromolecules*, **8**, 3973 (2007).
22. A. Jonathan, G. Milind, S. Sachiko, Y. Haihui, and H. Chen-ming, *Biomacromolecules*, **7**, 208 (2006).
23. A. Fraczek, E. Menaszek, C. Paluszkiewicz, and M. Blazewicz, *Acta Biomater.*, **4**, 1593 (2008).
24. M. Matsuoka, T. Akasaka, Y. Totsuka, and F. Watari, *Mat. Sci. Eng. B.*, **173**, 182 (2010).
25. S. Sofia, M. B. McCarthy, G. Gronowicz, and D. L. Kaplan, *Biomed. Mater.*, **54**, 139 (2001).
26. H. Xiao, D. L. Kaplan, and P. Cebe, *Macromolecular*, **39**, 6161 (2006).
27. Z. Wu, W. Feng, Y. Feng, Q. Liu, X. Xu, T. Sekino, A. Fujii, and M. Ozaki, *Carbon*, **45**, 1212 (2007).
28. J. L. Bahr, E. T. Mickelson, M. J. Bronikowski, R. E. Smalley, and J. M. Tour, *Chem. Commun.*, 193 (2001).
29. C. Tang, T. Zhou, J. Yang, Q. Zhang, F. Chen, Q. Fu, and L. Yang, *Colloid Surf. B-Biointerfaces*, **86**, 189 (2011).
30. A. Jonathan, G. Milind, S. Sachiko, and T. Haihui, *Biomacromolecules*, **7**, 208 (2006).